Article

IMM Fifth-Degree Spherical Simplex-Radial Cubature Filter for Maneuvering Target Tracking

Hua Liu * and Wen Wu

Ministerial Key Laboratory of JGMT, Nanjing University of Science and Technology, Nanjing 210094, China; wuwen@njust.edu.cn

* Correspondence: peterliuh@126.com; Tel.: +86-150-5184-1745

Abstract: For improving the tracking accuracy and model switching speed of maneuvering target tracking in nonlinear systems, a new algorithm named interacting multiple model fifth-degree spherical simplex-radial cubature filter (IMM5thSSRCKF) is proposed in this paper. The new algorithm is a combination of the interacting multiple model (IMM) filter and fifth-degree spherical simplex-radial cubature filter (5thSSRCKF). The proposed algorithm makes use of Markov process to describe the switching probability among the models, and uses 5thSSRCKF to deal with the state estimation of each model. The 5thSSRCKF is an improved filter algorithm, which utilizes the fifth-degree spherical simplex-radial rule to improve the filtering accuracy. Finally, the tracking performance of the IMM5thSSRCKF is evaluated by simulation in a typical maneuvering target tracking scenario. Simulation results show that the proposed algorithm has better tracking performance and quicker model switching speed when disposing maneuver models compared with IMMUKF, IMMCKF and IMM5thCKF.

Keywords: maneuvering target tracking; interacting multiple model; fifth-degree spherical simplex-radial rule; Markov process

1. Introduction

Maneuvering target tracking has been widely used in many applications, such as aircraft surveillance[1,2], road vehicle navigation [3,4] and radar tracking [5-7]. Because of the complexity of maneuvering target motion, the single model structure is not appropriate in tracking maneuvering targets. Therefore, the multiple-model structure is adopted. A number of multiple-model techniques have been proposed, such as multiple-model (MM) methods [8], optimization of multiple model neural filter [9],the interacting multiple-model (IMM) algorithm [10,11], and other algorithms [12,13]. In these multiple-model algorithms, the IMM algorithm proposed by Blom and Bar-Shalom [10,11] is the most popular algorithm. In the IMM algorithm, the target model is selected among a set of models via the control of a Markov chain and the final estimate is obtained by a weighted sum of the estimates from the sub-filters of different models. The conventional IMM algorithm combines multiple models with linear filter to estimate the target motion state. Because of its excellent compromise between complexity and performance, the IMM [8,14] algorithm has been widely used in the field of maneuvering target tracking [14-16]. However, in the conventional IMM algorithm, the Kalman filter only obtains high precision for linear Gaussian systems. But most modern systems are nonlinear and the linear IMM algorithm cannot directly deal with nonlinear systems. Thus the research of nonlinear IMM is paid more attention and is a popular topic in maneuvering target tracking field. It is different from linear IMM theory based on the linear Kalman filter, the performance of nonlinear IMM

Peer-reviewed version available at Sensors 2017, 17, , 1374; doi:10.3390/s17061374

algorithms depends on the selected nonlinear filters.

Nowadays, the study of nonlinear filter algorithm has been paid a great deal of attention by researchers. It is well known that the extended Kalman filter (EKF) [17] is widely used among the proposed nonlinear filtering algorithms. The basic idea of the EKF is to linearize the measurements and state models by the first order Taylor series expansion. However, it is difficult to get the Jacobian matrix of nonlinear function in many practical problems. As a result, the performance of the EKF may degrade rapidly. To solve this problem, scholars have proposed derivative-free alternatives such as the unscented Kalman filter (UKF) [18,19], the central difference Kalman filter (CDKF) [20] and the Gauss-Hermite Kalman filter (GHKF) [21], etc. These algorithms mentioned above use a set of deterministically sampling points and weights to approximate the Gaussian integrals, which are more accurate than the EKF. However, the search for more accurate filtering algorithms is continuing. In recent years, cubature Kalman filter (CKF) [22,23] is increasingly concerned for high-dimensional state estimation. This filtering algorithm approximates the weighted Gaussian integrals according to the Bayesian theory and the third degree spherical-radial cubature rule. With $2n$ equal weighted cubature points, the CKF performs more accurate and better numerical stability than the UKF.

To further improve the estimation accuracy of CKF the fifth-degree CKF (5thCKF) is proposed in [24]. However, the computational cost of the 5thCKF increases rapidly with the increasing of the state dimension. Recently, Wang et al. [25] have proposed a new class of CKF algorithms based on the spherical simplex-radial (SSR) rule, which can improve accuracy of the CKF with lower computational costs in high dimensional nonlinear system. Specially, the fifth-degree spherical simplex-radial cubature Kalman filter (5thSSRCKF) proposed in [25] has the higher estimation accuracy than 5thCKF. Therefore, we choose 5thSSRCKF as the filtering algorithm in the IMM framework, and propose interacting multiple model fifth-degree spherical simplex-radial cubature filter (IMM5thSSRCKF) algorithm for maneuvering target tracking of nonlinear system. Simulation results show that the IMM5thSSRCKF exhibits better performance than IMMUKF, IMMCKF and IMM5thCKF[26] in terms of accuracy and switching response.

The remainder of this paper is organized as follows. The fifth-degree spherical simplex-radial cubature Kalman filter is briefly reviewed in Section 2. The whole procession of IMM5thSSRCKF used in target tracking problem is developed in Section 3. Simulation results of a maneuvering tracking problem and performance comparisons are presented and discussed in Section 4. Finally, the conclusions are provided in Section 5.

2. Fifth-degree Simplex-Spherical Cubature Kalman Filter

The nonlinear filtering problem with additive process and measurement noise can be model by

$$\begin{cases} \boldsymbol{x}_k = \boldsymbol{f}\left(\boldsymbol{x}_{k-1}\right) + \boldsymbol{w}_{k-1} \\ \boldsymbol{z}_k = \boldsymbol{h}\left(\boldsymbol{x}_k\right) \quad + \boldsymbol{v}_k \end{cases} \tag{1}$$

where k is a discrete time index, $\boldsymbol{x}_k \in \mathbf{R}^n$ is the state vector at time k, $z_k \in \mathbf{R}^m$ is the measurement vector at time k; $\boldsymbol{f}(\cdot)$ and $\boldsymbol{h}(\cdot)$ are the system dynamics function and the measurement function; $\boldsymbol{w}_{k-1} \in \mathbf{R}^n$ is the process noise; $\boldsymbol{v}_k \in \boldsymbol{R}^m$ is the measurement noise. $\boldsymbol{w}_{k-1}$ and $\boldsymbol{v}_k$ are assumed to be uncorrelated zero-mean Gaussian white noise with covariance matrix $\boldsymbol{Q}_{k-1}$ and $\boldsymbol{R}_k$, respectively. The initial state $\boldsymbol{x}_0$ is assumed to be $\hat{\boldsymbol{x}}_0$ with covariance matrix $\boldsymbol{P}_0$ and is independent of $\boldsymbol{w}_{k-1}$ and $\boldsymbol{v}_k$.

2.1. Review of the fifth-degree spherical simplex-radial cubature rule

The 5thSSRCKF algorithm has the same structure as the general Gaussian approximation filters, such as the CKF, but uses the fifth-degree spherical simplex-radial cubature rule to calculate the Gaussian weight integral $\boldsymbol{I}(\boldsymbol{f}) = \int_{\mathbb{R}^n} \boldsymbol{f}(\boldsymbol{x}) N(\boldsymbol{x}; 0, \boldsymbol{I}) d\boldsymbol{x}$. By using the spherical simplex-radial cubature rule, the 5thSSRCKF method can get more accurate estimation than CKF. In the fifth-degree spherical simplex-radial cubature rule, the following integral is considered [24]:

$$\boldsymbol{I}(\boldsymbol{f}) = \int_{\mathbb{R}^n} \boldsymbol{f}(\boldsymbol{x}) \exp(-\boldsymbol{x}^{\mathrm{T}} \boldsymbol{x}) d\boldsymbol{x} \tag{2}$$

where $\boldsymbol{f}(\cdot)$ is arbitrary nonlinear function, $\mathbb{R}^n$ is the integral domain. To calculate the above integral, let $\boldsymbol{x} = r\boldsymbol{s}$ ($\boldsymbol{s}^T \boldsymbol{s} = 1, r = \sqrt{\boldsymbol{x}^{\mathrm{T}} \boldsymbol{x}}$). The Eq.(2) can be transformed into the spherical-radial coordinate system

$$\boldsymbol{I}(\boldsymbol{f}) = \int_0^{\infty} \int_{U_n} \boldsymbol{f}(r\boldsymbol{s}) r^{n-1} \exp(-r^2) d\sigma(\boldsymbol{s}) dr \tag{3}$$

where $\boldsymbol{s} = [s_1, s_2, \cdots, s_n]^{\mathrm{T}}$, $\boldsymbol{U}_n = \{\boldsymbol{s} \in \mathbb{R}^n : s_1^2 + s_2^2 + \cdots + s_n^2 = 1\}$ is the spherical surface, and $\sigma(\cdot)$ is the area element on $\boldsymbol{U}_n$. Then, the integral (3) can be decomposed into the spherical integral $\boldsymbol{S}(r) = \int_{U_n} \boldsymbol{f}(r\boldsymbol{s}) \mathrm{d}\sigma(\boldsymbol{s})$ and the radial integral $\boldsymbol{I}(\boldsymbol{f}) = \int_0^{\infty} \boldsymbol{S}(r) r^{n-1} \exp(-r^2) dr$.

2.1.1. Spherical simplex rule

As can be seen from [27], the spherical integral $\int_{U_n} \boldsymbol{f}(r\boldsymbol{s}) \mathrm{d}\sigma(\boldsymbol{s})$ can be approximated by the transformation group of the regular *n*-simplex. The fifth-degree spherical simplex rule with $n^2 + 3n + 2$ quadrature points is given by

$$\boldsymbol{S}_5(r) = \frac{(7-n)n^2 A_n}{2(n+1)^2 (n+2)^2} \sum_{j=1}^{n+1} \left[\boldsymbol{g}(r\boldsymbol{a}_j) + \boldsymbol{g}(-r\boldsymbol{a}_j) \right] + \frac{2(n-1)^2 A_n}{2(n+1)^2 (n+2)^2} \sum_{j=1}^{n(n+1)/2} \left[\boldsymbol{g}(r\boldsymbol{b}_j) + \boldsymbol{g}(-r\boldsymbol{b}_j) \right] \tag{4}$$

where $\boldsymbol{A}_n = 2\sqrt{\pi^n} / \Gamma^n(1/2)$ is the surface area of the unit sphere. The points sets of $\boldsymbol{a}_j$ and $\boldsymbol{b}_j$ are given by

$$\boldsymbol{a}_j = [a_{j,1}, a_{j,1}, \cdots, a_{j,n}]^T \tag{5}$$

$$\{\boldsymbol{b}_j\} = \left\{ \sqrt{\frac{n}{2(n-1)}} (\boldsymbol{a}_i + \boldsymbol{a}_l) : i < l; i, l = 1, 2, \cdots, n+1 \right\} \tag{6}$$

where the vector elements of $\boldsymbol{a}_j$ is defined as

$$a_{j,m} = \begin{cases} -\sqrt{\dfrac{n+1}{n(n-m+2)(n-m+1)}}, & m < j \\ \sqrt{\dfrac{(n+1)(n-j+1)}{n(n-j+2)}}, & m = j \\ 0, & m > j \end{cases}, \quad 1 \le m \le n, 1 \le j \le n+1 \tag{7}$$

2.1.2. Radial rule

The radial integral $R=\int_0^{\infty} S(r)r^{n-1}\exp(-r^2)dr$ can be calculated by the following moment matching equation

$$\int_0^{\infty} S(r)r^{n-1}\exp(-r^2)dr=\sum_{i=1}^{N_r}\omega_{r,i}S(r_i) \tag{8}$$

where $S(r)=r^l$ is a monomial in r, with l an even integer. The left-hand side of Equation (8) is simplified as $\frac{1}{2}\Gamma\left(\frac{n+l}{2}\right)$. In order to achieve the fifth-degree algebraic precision, we make the radial integral R is exact for l =0, 2, 4. For the fifth-degree radial rule $(N_r=2)$, we can obtain the moments' equations as

$$\begin{cases}\omega_{r,1}r_1^0+\omega_{r,2}r_2^0=\frac{1}{2}\Gamma\left(\frac{n}{2}\right)\\ \omega_{r,1}r_1^2+\omega_{r,2}r_2^0=\frac{1}{2}\Gamma\left(\frac{n+2}{2}\right)=\frac{n}{4}\Gamma\left(\frac{n}{2}\right)\\ \omega_{r,1}r_1^4+\omega_{r,2}r_2^4=\frac{1}{2}\Gamma\left(\frac{n+4}{2}\right)=\frac{1}{2}\left(\frac{n}{2}+1\right)\left(\frac{n}{2}\right)\Gamma\left(\frac{n}{2}\right)\end{cases} \tag{9}$$

By solving Eq.(9), the points and weights for the third-degree radial rule are given by

$$\begin{cases}r_1=0, & r_1=\sqrt{n/2+1}\\ \omega_{r,1}=\frac{1}{n+2}\Gamma(n/2), & \omega_{r,2}=\frac{n\Gamma(n/2)}{2(n+2)}\end{cases} \tag{10}$$

2.1.3. Fifth-degree spherical simplex-radial rule

By using Eqs.(3), (4) and (10), the fifth-degree spherical simplex-cubature rule can be formulated as

$$\begin{aligned}\int_{\mathbb{R}^n} g(\boldsymbol{x})N(\boldsymbol{x};\hat{\boldsymbol{x}},\boldsymbol{P}_x)d\boldsymbol{x}=&\frac{2}{n+2}g(\hat{\boldsymbol{x}})+\\ &\left\{\frac{(7-n)n^2}{2(n+1)^2(n+2)^2}\sum_{i=1}^{n+1}\left[g(\sqrt{(n+2)\boldsymbol{P}_x}\boldsymbol{a}_i+\hat{\boldsymbol{x}})+g(-\sqrt{(n+2)\boldsymbol{P}_x}\boldsymbol{a}_i+\hat{\boldsymbol{x}})\right]+\right.\\ &\left.\frac{2(n-1)^2}{2(n+1)^2(n+2)^2}\sum_{i=1}^{n(n+1)/2}\left[g(\sqrt{(n+2)\boldsymbol{P}_x}\boldsymbol{b}_i+\hat{\boldsymbol{x}})+g(-\sqrt{(n+2)\boldsymbol{P}_x}\boldsymbol{b}_i+\hat{\boldsymbol{x}})\right]\right\}\end{aligned} \tag{11}$$

The steps of 5thSSRCKF algorithm for the nonlinear system can be found in [22] and [25].

3. IMM5thSSRCKF algorithm

The proposed IMM5thSSRCKF algorithm is the combination of IMM algorithm and 5thSSRCKF algorithm. In the IMM5thSSRCKF algorithm, the state estimation at time k is computed under each possible current model using r filters, with each filter using a different combination of the previous model-conditioned estimates. The structure diagram of IMM5thSSRCKF is shown in Fig.1.

Preprints (www.preprints.org) | NOT PEER-REVIEWED | Posted: 18 April 2017 doi:10.20944/preprints201704.0106.v1

Peer-reviewed version available at Sensors 2017, 17, , 1374; doi:10.3390/s17061374

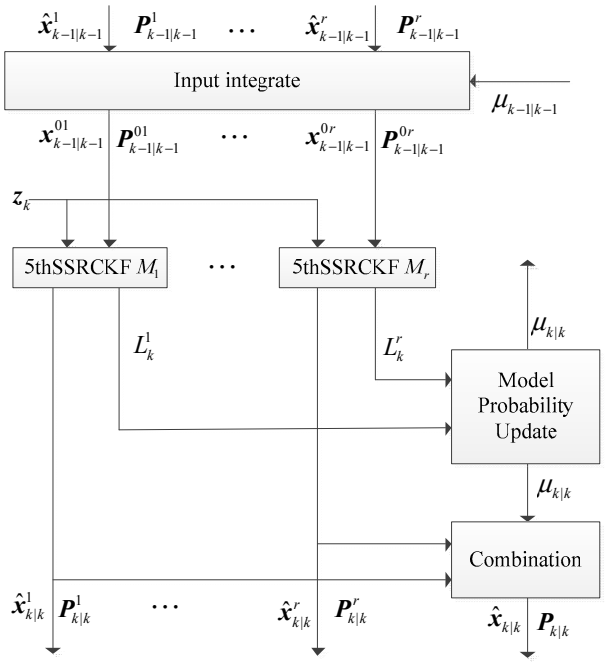

Figure 1. Structure of IMM5thSSRCKF

In the IMM5thSSRCKF algorithm, the 5thSSRCKF employs the fifth-degree spherical simplex-radial cubature rule to generate the cubature points, which can further estimate the mean and covariance of the system state. The IMM5thSSRCKF algorithm includes four fundamental steps: model interaction, model conditional filtering, model probability updating, and output integration. The detailed steps of the IMM5thSSRCKF algorithm are provided as follows.

Step 1. *Model interaction*

The initial condition for each model j can be obtained from the state estimate $\hat{\boldsymbol{x}}^{j}_{k-1|k-1}$ and covariance $\boldsymbol{P}^{j}_{k-1|k-1}$ at time $k-1$. The mixed initial state of model j at time $k-1$ $\hat{\boldsymbol{x}}^{0j}_{k-1|k-1}$ and its corresponding covariance $\boldsymbol{P}^{0j}_{k-1|k-1}$ are computed according to

$$\begin{aligned}\hat{\boldsymbol{x}}^{0j}_{k-1|k-1} &= \sum_{i=0}^{r}\mu^{i|j}_{k-1|k-1}\hat{\boldsymbol{x}}^{i}_{k-1|k-1}\\ \boldsymbol{P}^{0j}_{k-1|k-1} &= \sum_{i=0}^{r}\mu^{i|j}_{k-1|k-1}\{\boldsymbol{P}^{i}_{k-1|k-1}+\left[\hat{\boldsymbol{x}}^{i}_{k-1|k-1}-\hat{\boldsymbol{x}}^{0j}_{k-1|k-1}\right]\left[\hat{\boldsymbol{x}}^{i}_{k-1|k-1}-\hat{\boldsymbol{x}}^{0j}_{k-1|k-1}\right]^{T}\}\end{aligned} \tag{12}$$

where r denotes the number of interacting models, $\hat{\boldsymbol{x}}^{i}_{k-1|k-1}$ and $\boldsymbol{P}^{i}_{k-1|k-1}$ are the prior state estimate and corresponding state error covariance of model i in the previous step, respectively.

The mixing probability $\mu^{i|j}_{k-1|k-1}$ at time $k-1$ can be given by

$$\begin{aligned}\mu^{i|j}_{k-1} &= \frac{p_{ij}\mu^{i}_{k-1}}{C_j},\\ C_j &= \sum_{i=1}^{r}p_{ij}\mu^{i}_{k-1}\end{aligned} \tag{13}$$

where $i,j=1,\cdots,r$, μ^{i}_{k-1} represents the model probability of the mode i at time k-1, and p_{ij} is the probability of a transition from model i to model j.

Step 2. *Model conditional filtering*

Using the initial mixing state $\boldsymbol{x}^{0j}_{k-1|k-1}$ and the covariance $\boldsymbol{P}^{0j}_{k-1|k-1}$ of the interacting step as the

Peer-reviewed version available at Sensors 2017, 17, , 1374; doi:10.3390/s17061374

input of each filter at time $k-1$. Then the new state $\hat{\boldsymbol{x}}_{k|k}^{j}$ of model j and covariance $\boldsymbol{P}_{k|k}^{j}$ of model j can be updated by Eq.(14)~Eq.(20).

A. Time Update

The evaluation of cubature points in the mechanism of state one-step prediction and the propagated cubature points in the mechanism of state one-step prediction can be obtained by the following equations:

$$\begin{aligned} \boldsymbol{X}_{i,k|k-1}^{j} &= \boldsymbol{S}_{k-1|k-1}^{0j}\boldsymbol{\xi}_{i}^{j} + \boldsymbol{x}_{k-1|k-1}^{0j} \\ \boldsymbol{X}_{i,k|k-1}^{*j} &= \boldsymbol{f}(\boldsymbol{X}_{i,k|k-1}^{j}) \end{aligned} \tag{14}$$

where $\boldsymbol{S}_{k-1|k-1}^{0j}$ is the square root factor of $\boldsymbol{P}_{k-1|k-1}^{0j}$ and $\boldsymbol{P}_{k-1|k-1}^{0j}$ is the estimated error covariance of model j at time $k-1$, $\{\boldsymbol{\xi}_{i}^{j}\}$ is the matrix with a set of vector, and the corresponding weight matrix is $\{\omega_{i}^{j}\}$. The fifth-degree simplex cubature points and the corresponding weights are as follows:

$$\boldsymbol{\xi}_{i}^{j} = \begin{cases} [0,0,\cdots,0]^{T} & i=1, \\ \sqrt{n+2}\,\boldsymbol{a}_{i-1} & i=2,\cdots,n+2, \\ -\sqrt{n+2}\,\boldsymbol{a}_{i-n-2} & i=n+3,\cdots,2n+3, \\ \sqrt{n+2}\,\boldsymbol{b}_{i-2n-3} & i=2n+4,\cdots,(n^{2}+5n+6)/2, \\ -\sqrt{n+2}\,\boldsymbol{b}_{i-(n^{2}+5n+6)/2} & i=(n^{2}+5n+8)/2,\cdots,n^{2}+3n+3. \end{cases} \tag{15}$$

$$\omega_{i}^{j} = \begin{cases} \dfrac{2}{n+2} & i=1, \\ \dfrac{(7-n)n^{2}}{2(n+1)^{2}(n+2)^{2}} & i=2,\cdots,2n+3, \\ \dfrac{2(n-1)^{2}}{n(n+1)^{2}(n+2)^{2}} & i=2n+4,\cdots,n^{2}+3n+3. \end{cases} \tag{16}$$

where n represents the dimension of state vector, the point sets of $\boldsymbol{a}_{i}$ and $\boldsymbol{b}_{i}$ are given by (5) and (6).

The predicted state $\boldsymbol{x}_{k|k-1}^{j}$ and predicted error covariance $\boldsymbol{P}_{k|k-1}^{j}$ can be computed using the cubature transformation as

$$\begin{aligned} \boldsymbol{x}_{k|k-1}^{j} &= \sum_{i=1}^{L}\omega_{i}\boldsymbol{X}_{i,k|k-1}^{*j} \\ \boldsymbol{P}_{k|k-1}^{j} &= \sum_{i=1}^{L}\omega_{i}(\boldsymbol{X}_{i,k|k-1}^{*j} - \boldsymbol{x}_{k|k-1}^{j})(\boldsymbol{X}_{i,k|k-1}^{*j} - \boldsymbol{x}_{k|k-1}^{j})^{T} + \boldsymbol{Q}_{k-1} \end{aligned} \tag{17}$$

where the number of points L is $n^{2}+3n+3$, $\boldsymbol{Q}_{k-1}$ denotes the system noise covariance matrix.

B. Measurement Update

The cubature points used for the measurement update and the propagated cubature points are derived as

$$\begin{aligned} \boldsymbol{\chi}_{i,k|k-1}^{j} &= \boldsymbol{S}_{k|k-1}^{j}\boldsymbol{\xi}_{i}^{j} + \boldsymbol{x}_{k|k-1}^{j} \\ \boldsymbol{Z}_{i,k|k-1}^{j} &= h(\boldsymbol{\chi}_{i,k|k-1}^{j}) \end{aligned} \tag{18}$$

where $\boldsymbol{S}_{k|k-1}^{j}$ can be obtained by factorizing the predicted error covariance $\boldsymbol{P}_{k|k-1}^{j}$.

The prediction value of the measurement vector $\boldsymbol{z}_{k|k-1}^{j}$, the innovation covariance matrix $\boldsymbol{P}_{zz,k|k-1}^{j}$,

Preprints (www.preprints.org) | NOT PEER-REVIEWED | Posted: 18 April 2017 doi:10.20944/preprints201704.0106.v1

Peer-reviewed version available at Sensors 2017, 17, , 1374; doi:10.3390/s17061374

and the cross covariance matrix $\boldsymbol{P}^{j}_{xz,k|k-1}$ are given as follows

$$\begin{aligned}
\boldsymbol{z}^{j}_{k|k-1} &= \sum_{i=1}^{L} \omega_i \boldsymbol{Z}^{j}_{i,k|k-1} \\
\boldsymbol{P}^{j}_{zz,k|k-1} &= \sum_{i=1}^{L} \omega_i (\boldsymbol{Z}^{j}_{i,k|k-1} - \boldsymbol{z}^{j}_{k|k-1})(\boldsymbol{Z}^{j}_{i,k|k-1} - \boldsymbol{z}^{j}_{k|k-1})^{T} + \boldsymbol{R} \\
\boldsymbol{P}^{j}_{xz,k|k-1} &= \sum_{i=1}^{L} \omega_i (\boldsymbol{\chi}^{j}_{i,k|k-1} - \boldsymbol{x}^{j}_{k|k-1})(\boldsymbol{Z}^{j}_{i,k|k-1} - \boldsymbol{z}^{j}_{k|k-1})^{T}
\end{aligned} \tag{19}$$

Finally, the estimated state $\hat{\boldsymbol{x}}^{j}_{k|k}$ of model j and the estimated error covariance $\boldsymbol{P}^{j}_{k|k}$ of model j can be derived as follows

$$\begin{aligned}
\boldsymbol{K}^{j}_{k} &= \boldsymbol{P}^{j}_{xz,k|k-1} \cdot \mathrm{inv}(\boldsymbol{P}^{j}_{zz,k|k-1}) \\
\hat{\boldsymbol{x}}^{j}_{k|k} &= \boldsymbol{x}^{j}_{k|k-1} + \boldsymbol{K}^{j}_{k}(z_k - \boldsymbol{z}^{j}_{k|k-1}) \\
\boldsymbol{P}^{j}_{k|k} &= \boldsymbol{P}^{j}_{k|k-1} - \boldsymbol{K}^{j}_{k}\boldsymbol{P}^{j}_{zz,k|k-1}(\boldsymbol{K}^{j}_{k})^{T}
\end{aligned} \tag{20}$$

Step 3. *Update the mode probability at time* k

A Compute the likelihood function at time k

With the use of the latest measurement z_k, the likelihood function value of model j at time k is given by

$$\boldsymbol{L}^{j}_{k} = N(\boldsymbol{z}_k; \boldsymbol{z}^{j}_{k|k-1}, v^{j}_{k}) = \left|2\pi \boldsymbol{S}^{(j)}_{k}\right|^{-n_z/2} \exp\left\{-\frac{1}{2}[z_k - \boldsymbol{z}^{j}_{k|k-1}]^{T}(\boldsymbol{S}^{(j)}_{k})^{-1}[z_k - \boldsymbol{z}^{j}_{k|k-1}]\right\} \tag{21}$$

where $v^{j}_{k} = z_k - \boldsymbol{z}^{j}_{k|k-1}$ denotes the filter residual and $\boldsymbol{S}^{(j)}_{k}$ denotes the innovation covariance and n_z denotes the dimension of measurement vector.

B Update the mode probability at time k

The mode probability $\mu^{j}_{k|k}$ at time k is computed by the following equation

$$\mu^{j}_{k|k} = \frac{\boldsymbol{L}^{j}_{k} C_j}{\boldsymbol{C}}, \quad \boldsymbol{C} = \sum_{i=1}^{r} \boldsymbol{L}^{j}_{k} C_i \tag{22}$$

Step 4. *Output integration*

Finally, the state estimate $\hat{\boldsymbol{x}}_{k|k}$ and corresponding covariance $\boldsymbol{P}_{k|k}$ are obtained by the model-conditional estimates and covariances of different models

$$\hat{\boldsymbol{x}}_{k|k} = \sum_{j=1}^{r} \mu^{j}_{k|k} \hat{\boldsymbol{x}}^{j}_{k|k} \tag{23}$$

$$\boldsymbol{P}_{k|k} = \sum_{j=1}^{r} \mu^{j}_{k|k} \left\{ \boldsymbol{P}^{j}_{k|k} + \left[\hat{\boldsymbol{x}}^{j}_{k|k} - \hat{\boldsymbol{x}}_{k|k}\right]\left[\hat{\boldsymbol{x}}^{j}_{k|k} - \hat{\boldsymbol{x}}_{k|k}\right]^{T} \right\} \tag{24}$$

4. Simulation and results

To validate the performance of the proposed algorithm, a highly maneuvering target example has been considered. The proposed algorithm will be compared with the IMMCKF, IMMUKF, and IMM5thCKF algorithm.

4.1. Tracking model and measurement model

Let the state vector at time k be $\boldsymbol{x}_k = [x_k, \dot{x}_k, y_k, \dot{y}_k]^{T}$, which includes the position (m) and velocity component (m/s) in x-axis and y-axis. For tracking of the maneuvering target, three models are employed: constant velocity (CV) model, left constant turn (LCT) model and right constant turn (RCT) model. For constant velocity model, the equation of state is described as

Peer-reviewed version available at Sensors 2017, 17, , 1374; doi:10.3390/s17061374

$$\boldsymbol{x}_k = \boldsymbol{F}_{\mathrm{CV}}\boldsymbol{x}_{k-1} + \boldsymbol{G}_{\mathrm{CV}}w_{\mathrm{CV}}; \tag{25}$$

$$\boldsymbol{F}_{\mathrm{CV}} = \begin{bmatrix} 1 & T & 0 & 0 \\ 0 & 1 & 0 & 0 \\ 0 & 0 & 1 & T \\ 0 & 0 & 0 & 1 \end{bmatrix};\ \boldsymbol{G}_{\mathrm{CV}} = \begin{bmatrix} T^2/2 & 0 \\ T & 0 \\ 0 & T^2/2 \\ 0 & T \end{bmatrix} \tag{26}$$

where w_{CV} is the process noise vector with a zero-mean Gaussian white noise and with a standard deviation [10, 0; 0, 10].

The constant turn (CT) model is defined as

$$\boldsymbol{x}_k = \boldsymbol{F}_{\mathrm{CT}}\boldsymbol{x}_{k-1} + \boldsymbol{G}_{\mathrm{CT}}w_{\mathrm{CT}}; \tag{27}$$

$$\boldsymbol{F}_{\mathrm{CT}} = \begin{bmatrix} 1 & \dfrac{\sin\omega T}{\omega} & 0 & -\left(\dfrac{1-\cos\omega T}{\omega}\right) \\ 0 & \cos\omega T & 0 & -\sin\omega T \\ 0 & \dfrac{1-\cos\omega T}{\omega} & 1 & \dfrac{\sin\omega T}{\omega} \\ 0 & \sin\omega T & 0 & \cos\omega T \end{bmatrix};\ \boldsymbol{G}_{\mathrm{CT}} = \begin{bmatrix} T^2/2 & 0 \\ T & 0 \\ 0 & T^2/2 \\ 0 & T \end{bmatrix} \tag{28}$$

where T is the sampling interval, ω stands for the turn rate which is supposed to be known, the right turn rate is defined as $-3°$, and the left turn rate is defined as $3°$. w_{CV} is the process noise vector with a zero-mean Gaussian white noise and with a standard deviation [15, 0; 0, 15].

In the experiment, the radar is located at the origin of the plan and equipped to measure range and bearing. Then, the measurement equation can be written as

$$\boldsymbol{z}_k = \begin{pmatrix} r_k \\ \theta_k \end{pmatrix} = \begin{pmatrix} \sqrt{x_k^2 + y_k^2} \\ \mathrm{atan2}(y_k, x_k) \end{pmatrix} + \boldsymbol{v}_k \tag{29}$$

where r_k is the range value, ϕ_k is the bearing value, atan2(·) is the four-quadrant inverse tangent function, $\boldsymbol{v}_k$ is the white Gaussian measurement noise with zero mean and covariance $\boldsymbol{R}_k = diag([\sigma_r^2, \sigma_\theta^2])$. σ_r and σ_θ denote the standard deviation of range measurement noise and bearing angle measurement noise, respectively.

4.2. Simulation of the IMM5thSSRCKF

The simulation scene is designed as follows. The sampling interval is T=1 s and repeat for 100 times. The target moves in different state for five periods. The initial position is (15000 m, 1000 m) and the target starts at time 1 s with the velocity (-180 m/s, 200 m/s). From time 1 s to time 20 s it does constant velocity motion; from time 21 s to time 40 s it turns right with $\omega = -3°$; from time 41 s to 60 s it does constant velocity motion; from time 61 s to 80 s it maneuvers and turns left with $\omega = 3°$; from time 81 s to 100 s it does constant velocity motion.

The initial estimate $\hat{\boldsymbol{x}}_0$ are generated from the Gaussian distribution $\boldsymbol{N}(\hat{\boldsymbol{x}}_0; \boldsymbol{x}_0, \boldsymbol{P}_0)$ in which the true initial is $\boldsymbol{x}_0$ =[15000, -180, 100, 200]^T. The standard deviation of range measurement noise σ_r is 40 m and the standard deviation of bearing angle measurement noise σ_θ is 7 mrad. The initial model probability is μ = [0.8 0.1 0.1] and the transition probability is given as

$$p_{ij} = \begin{bmatrix} 0.95 & 0.025 & 0.025 \\ 0.025 & 0.95 & 0.025 \\ 0.025 & 0.025 & 0.95 \end{bmatrix} \tag{30}$$

The RMSE of the target position at time k and the accumulative RMSE (ARMSE) of estimated

Preprints (www.preprints.org) | NOT PEER-REVIEWED | Posted: 18 April 2017 doi:10.20944/preprints201704.0106.v1

Peer-reviewed version available at Sensors 2017, 17, , 1374; doi:10.3390/s17061374

position at all times are defined in Eqs. (31) and (32)

$$\mathrm{RMSE}_{\mathrm{pos}}(k)=\sqrt{\frac{1}{M}\sum_{m=1}^{M}((x_k-\hat{x}_{m,k})^2+(y_k-\hat{y}_{m,k})^2)} \tag{31}$$

$$\mathrm{ARMSE}_{\mathrm{pos}}=\sqrt{\frac{1}{N}\sum_{k=1}^{N}(\mathrm{RMSE}_{\mathrm{pos}}^2(k))} \tag{32}$$

where M is the number of Monte Carlo runs, (x_k, y_k) is the actual value of the target position at time k and $(\hat{x}_{m,k}, \hat{y}_{m,k})$ is the estimated position at time k in mth Monte-Carlo. The RMSE and the accumulative RMSE in the velocity and acceleration can be defined in the same way. The performance comparison of the four algorithms are tested by 200 times Monte Carlo simulations.

Figure 2 gives the target trajectory and the state estimation generated from a single run of IMMUKF, IMMCKF, IMM5thCKF and IMM5thSSRCKF. As seen from Figure 2, these four algorithms can track the trajectory of the target.

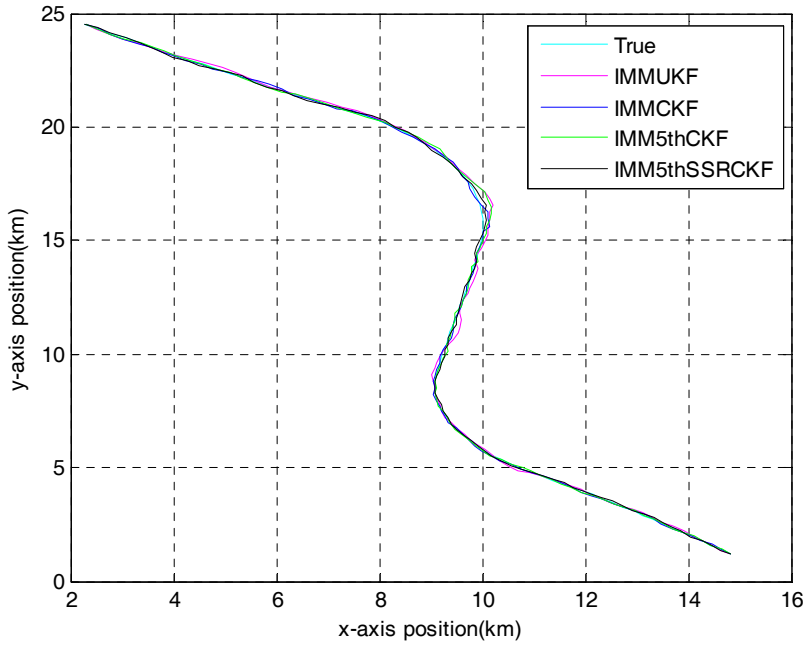

Figure 2. Trajectory of maneuvering target

The RMSEs in position and velocity of the four algorithms are shown in Figs.3 and 4, respectively. It can be seen that the proposed IMM5thSSRCKF performs better than the IMMUKF, IMMCKF and IMM5thCKF algorithms when the target moves with CV. The tracking error of target position of the three IMM algorithms would be almost the same when the target moves at constant velocity. The estimation effectiveness of the IMM5thSSRCKF estimator for tracking a maneuvering target outperform greatly than the other two IMM estimators.

Peer-reviewed version available at Sensors 2017, 17, , 1374; doi:10.3390/s17061374

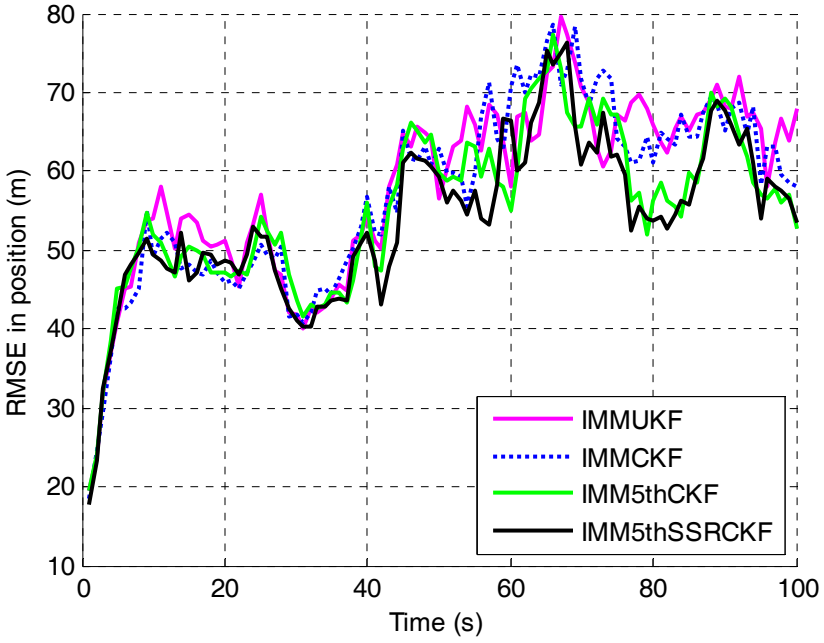

Figure 3. RMSE in position versus time step

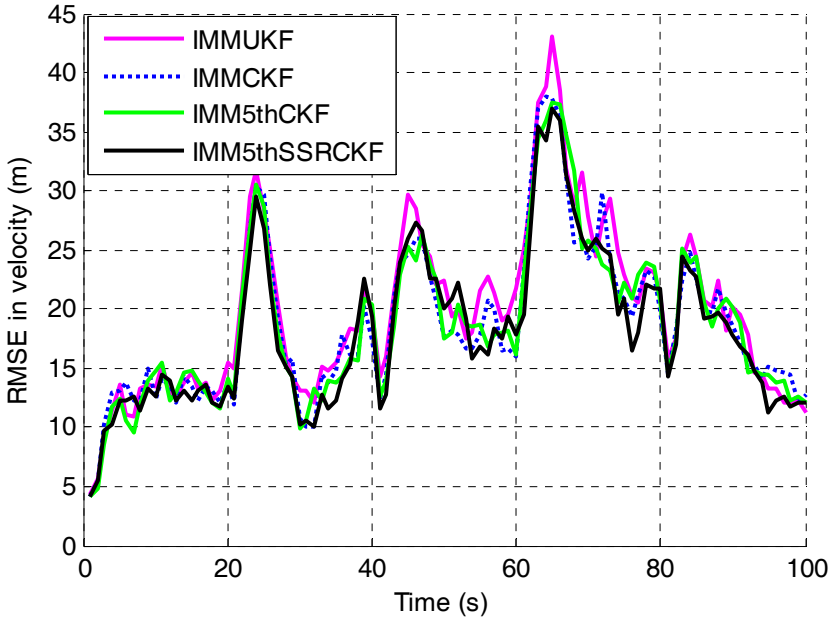

Figure 4. RMSE in velocity versus time step

To further evaluate the performance of the four algorithms, the ARMSEs of position and velocity of each algorithm are listed in Table 1. It can be seen from the Table1 that IMM5thSSRCKF does better in tracking precision than IMMUKF, IMMCKF and IMM5thCKF, while all of them exhibit no error divergence.

Peer-reviewed version available at Sensors 2017, 17, , 1374; doi:10.3390/s17061374

Table 1. Comparisons of ARMSE among the four algorithms

Filters	Position ARMSE/m	Velocity ARMSE/(m/s)
IMMUKF	61.1	22.3
IMMCKF	57.3	21.4
IMM5thCKF	54.7	19.4
IMM5thSSRCKF	52.5	18.3

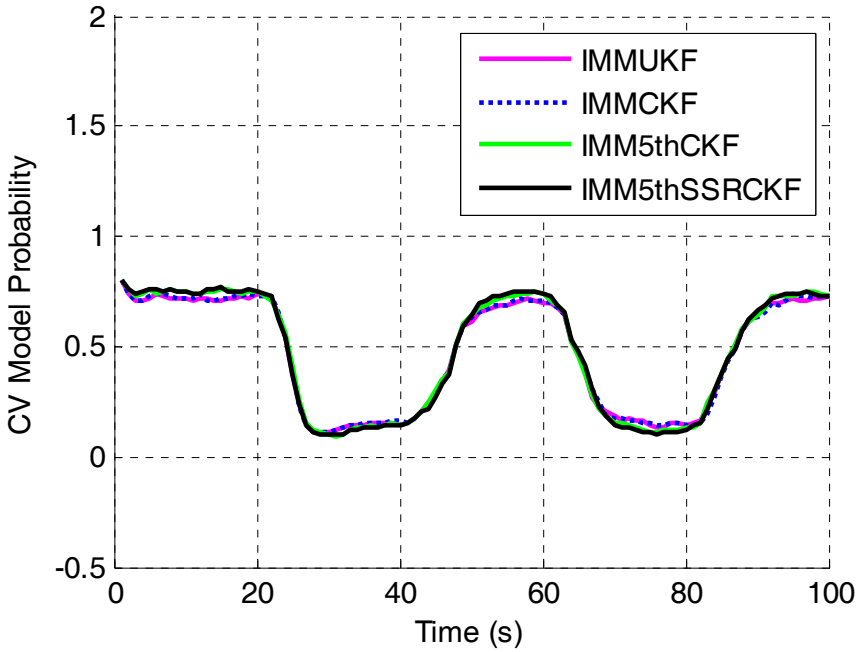

Figure 5. CV mode probability versus time step.

The comparisons of CV mode probability of IMMUKF, IMMCKF, IMM5thCKF and IMM5thSSRCKF are shown in Figure 5. The mode transitions occur at t = 21 s, t = 41 s, t = 61 s and t = 81 s, respectively. This figure shows that the IMMUKF, IMMCKF, IMM5thCKF and IMM5thSSRCKF can capture the kinematics of maneuvering when the motion state changes. And it can be seen that the mode probabilities of the IMMUKF algorithm is not good in detecting mode transitions. The proposed algorithm and IMM5thCKF algorithm are equally faster in detecting model changes compared with the IMMUKF algorithm and the IMMCKF algorithm.

Table 2. Number of points and computational time of different algorithms

Filters	Number of points(n=4)	Computational Time (s)
IMMUKF	9	0.128
IMMCKF	8	0.135
IMM5thCKF	33	0.311
IMM5thSSRCKF	31	0.293

All the algorithms are implemented on the Intel Core(TM) i5-4430 3.0GHZ CPU with 4.00G RAM. Table 2 shows the number of points and computational time of IMMUKF, IMMCKF, IMM5thCKF and IMM5thSSRCKF for each run. The points of IMMCKF as well as IMMUKF differs only by one points. As shown in Table 2, the computational time of the algorithms is approximately proportional to the number of points. It is obvious that the IMM5thSSRCKF algorithm has a slightly lower computational

cost than IMM5thCKF due to the different cubature rule. Although the IMM5thSSRCKF needs more computational time than the IMMUKF and IMMCKF, considering the performance improvement, this increased computational time is worth it.

5. Conclusion

In this paper, a new maneuvering target tracking algorithm named IMM5thSSRCKF is proposed to improve the tracking accuracy for maneuvering target. The proposed algorithm introduces the 5thSSRCKF algorithm into the IMM framework. The performance of the proposed algorithm is evaluated by simulations and compared with IMMUKF, IMMCKF and IMM5thCKF. Simulation results show that the IMM5thSSRCKF algorithm gets higher tracking accuracy than IMMUKF, IMMCKF and IMM5thCKF algorithms.

References

1 Cho, T.; Lee, C.; Choi, S. "Multi-Sensor fusion with interacting multiple model filter for improved aircraft position accuracy," *sensors* ***2013***, 13, 4122-4137, DOI:10.3390/s130404122. Available: <Go to ISI>://000318036400009.

2 Ehrman, L.M.; Lanterman, A.D. "Extended Kalman filter for estimating aircraft orientation from velocity measurements," *IET Radar, Sonar and Navigation* ***2008***, 2, 12-16, DOI:10.1049/iet-rsn:20070025. Available: http://dx.doi.org/10.1049/iet-rsn:20070025.

3 Oh, H.; Shin, H.S.; Kim, S.; Tsourdos, A.; White, B.A. "Airborne behaviour monitoring using Gaussian processes with map information," *IET Radar Sonar and Navigation* ***2013***, 7, 393-400, DOI:10.1049/iet-rsn.2012.0255. Available: <Go to ISI>://000322799100007.

4 Toledo-Moreo, R.; Zamora-Izquierdo, M.A.; Ubeda-Miarro, B.; Gomez-Skarmeta, A.F. "High-Integrity IMM-EKF-based road vehicle navigation with low-cost GPS/SBAS/INS," *IEEE Trans. Intell. Transp. Syst.* ***2007***, 8, 491-511, DOI:10.1109/tits.2007.902642. Available: <Go to ISI>://WOS:000249403800012.

5 Zhu, Z.W. "Shipborne radar maneuvering target tracking based on the variable structure adaptive grid interacting multiple model," *Journal of Zhejiang University-Science C-Computers & Electronics* ***2013***, 14, 733-742, DOI:10.1631/jzus.C1200335. Available: <Go to ISI>://000324103700006.

6 Arulampalam, M.S.; Ristic, B.; Gordon, N.; Mansell, T. "Bearings-only tracking of manoeuvring targets using particle filters," *Eurasip Journal on Applied Signal Processing* ***2004***, 2004, 2351-2365, DOI:Doi 10.1155/S1110865704405095. Available: <Go to ISI>://000226465700011.

7 Li, W.; Liu, M.H.; Duan, D.P. "Improved robust Huber-based divided difference filtering," *Proceedings of the Institution of Mechanical Engineers Part G-Journal of Aerospace Engineering* ***2014***, 228, 2123-2129, DOI:10.1177/0954410013507414. Available: <Go to ISI>://000342798900016.

8 Li, X.R.; Jilkov, V.P. "Survey of maneuvering target tracking. Part V: Multiple-model methods," *IEEE Trans. Aero. Elec. Syst.* ***2005***, 41, 1255-1321. Available: <Go to ISI>://000234232800007.

9 Kazimierski, W.; Stateczny, A. "Optimization of multiple model neural tracking filter for marine targets," *13th International Radar Symposium (IRS)*, Warsaw, Poland; K. Kulpa, 2012, pp. 543-548.

10 Blom, H.A.P.; Bar-Shalom, Y. "The interacting multiple model algorithm for systems with Markovian switching coefficients," *IEEE Trans. Automat. Contr.* ***1988***, 33, 780-783, DOI:10.1109/9.1299.

11 Bar-Shalom, Y.; Challa, S.; Blom, H.A.P. "IMM estimator versus optimal estimator for hybrid systems," *IEEE Trans. Aero. Elec. Syst.* ***2005***, 41, 986-991, DOI:10.1109/TAES.2005.1541443

12 Munir, A.; Atherton, D.P. "Adaptive interacting multiple model algorithm for tracking a manoeuvring target," *IEE Proceedings - Radar, Sonar and Navigation* ***1995***, 142, 11-17, DOI:10.1049/ip-rsn:19951528.

13 Lee, B.J.; Park, J.B.; Lee, H.J.; Joo, Y.H. "Fuzzy-logic-based IMM algorithm for tracking a manoeuvring target," *IEE Proceedings-Radar, Sonar and Navigation* ***2005***, 152, 16-22, DOI:10.1049/ip-rsn:20041002. Available: http://dx.doi.org/10.1049/ip-rsn:20041002.

14 Mazor, E.; Averbuch, A.; Bar-Shalom, Y.; Dayan, J. "Interacting multiple model methods in target tracking: a survey," *IEEE Transactions on Aerospace and Electronic Systems* ***1998***, 34, 103-123, DOI:10.1109/7.640267.

15 Qu, H.Q.; Pang, L.P.; Li, S.H. "A novel interacting multiple model algorithm," *Signal Processing* ***2009***, 89, 2171-2177, DOI:10.1016/j.sigpro.2009.04.033. Available: <Go to ISI>://000268425000009.

16 Gao, L.; Xing, J.P.; Ma, Z.L.; Sha, J.C.; Meng, X.Z. "Improved IMM algorithm for nonlinear maneuvering target tracking," *Procedia Engineering* ***2012***, 29, 4117-4123, DOI:10.1016/j.proeng.2012.01.630. Available: <Go to ISI>://000314346404029.

17 Kim, B.; Yi, K.; Yoo, H.J.; Chong, H.J.; Ko, B. "An IMM/EKF approach for enhanced multitarget state estimation for application to integrated risk management system," *IEEE Trans. Veh. Technol.* ***2015***, 64, 876-889, DOI:10.1109/Tvt.2014.2329497. Available: <Go to ISI>://000351459600003.

18 Julier, S.J.; Uhlmann, J.K. "Unscented filtering and nonlinear estimation," *Proc. IEEE* ***2004***, 92, 401-422.

19 Julier, S.J.; Uhlmann, J.K.; Durrant-Whyte, H.F. "A new method for the nonlinear transformation of means and covariances in filters and estimators," *IEEE Trans. Automat. Contr.* ***2000***, 45, 477-82, DOI:10.1109/9.847726. Available: http://dx.doi.org/10.1109/9.847726.

20 Ito, K.; Xiong, K.Q. "Gaussian filters for nonlinear filtering problems," *IEEE Trans. Automat. Contr.* ***2000***, 45, 910-927. Available: <Go to ISI>://000088530500007.

21 Arasaratnam, I.; Haykin, S.; Elliott, R.J. "Discrete-time nonlinear filtering algorithms using Gauss-Hermite quadrature," *Proc. IEEE* ***2007***, 95, 953-977. Available: <Go to ISI>://000247985500007.

22 Arasaratnam, I.; Haykin, S. "Cubature Kalman filters," *IEEE Trans. Automat. Contr.* ***2009***, 54, 1254-1269, DOI:10.1109/tac.2009.2019800. Available: http://dx.doi.org/10.1109/TAC.2009.2019800.

23 Arasaratnam, I.; Haykin, S. "Cubature Kalman smoothers," *Automatica* ***2011***, 47, 2245-2250, DOI:10.1016/j.automatica.2011.08.005. Available: http://dx.doi.org/10.1016/j.automatica.2011.08.005.

24 Jia, B.; Xin, M.; Cheng, Y. "High-degree cubature Kalman filter," *Automatica* ***2013***, 49, 510-518. Available: <Go to ISI>://000315003100022.

25 Wang, S.Y.; Feng, J.C.; Tse, C.K. "Spherical simplex-radial cubature Kalman filter," *IEEE Signal Proc. Let.* ***2014***, 21, 43-46. Available: <Go to ISI>://000327503000002.

26 Zhu, W.; Wang, W.; Yuan, G.N. "An improved interacting multiple model filtering algorithm based on the cubature Kalman filter for maneuvering target tracking," *Sensors* ***2016***, 16, DOI:10.3390/S16060805. Available: <Go to ISI>://WOS:000378756500053.

27 Jia, B.; Xin, M. "Multiple sensor estimation using a new fifth-degree cubature information filter," *T. I. Meas. Control* ***2015***, 37, 15-24, DOI:10.1177/0142331214523032. Available: <Go to ISI>://WOS:000346645400002.